Supplementary Materials

Supplementary Figures	
Supplementary Figure 1	Structural differences between the S1 domain of SARS-CoV-2 and endemic strains.
Supplementary Figure 2	IgA and IgM responses in the DHMC cohort.
Supplementary Figure 3	Antibody responses in the JHMI cohort.
Supplementary Figure 4	Elevated IgG but not IgM responses to endemic CoV in convalescent cohorts.
Supplementary Figure 5	Elevated responses to endemic CoV in the pre- and post-infection cohort.
Supplementary Figure 6	Correlative relationships between SARS-CoV-2- and OC43-specific antibody responses in the JHMI cohort by isotype.
Supplementary Figure 7	Cross-reactivity of SARS-CoV-2 S-2P specific IgG.
Supplementary Figure 8	Cross-reactivity of SARS-CoV-2 RBD specific IgG.
Supplementary Figure 9	Cross-reactivity of SARS-CoV-2 S2 specific IgG.
Supplementary Figure 10	Cross-reactivity of OC43 S specific IgG.
Supplementary Figure 11	Cross-reactivity of SARS-CoV-2 S-2P specific IgA.
Supplementary Figure 12	Cross-reactivity of SARS-CoV-2 RBD specific IgA.
Supplementary Figure 13	Cross-reactivity of SARS-CoV-2 S2 specific IgA.
Supplementary Figure 14	Cross-reactivity of OC43 S specific IgA.
Supplementary Figure 15	Cross-reactivity of SARS-CoV-2 S-2P specific IgM.
Supplementary Figure 16	Cross-reactivity of SARS-CoV-2 RBD specific IgM.
Supplementary Figure 17	Cross-reactivity of SARS-CoV-2 S2 specific IgM.
Supplementary Figure 18	Cross-reactivity of OC43 S specific IgM.
Supplementary Figure 19	IgA and IgM responses among naïve subjects, infected pregnant women, vaccinated adults, and vaccinated pregnant women.
Supplementary Tables	
Supplementary Table 1	Coronavirus structures.
Supplementary Table 2	Fc detection and antigen reagents.

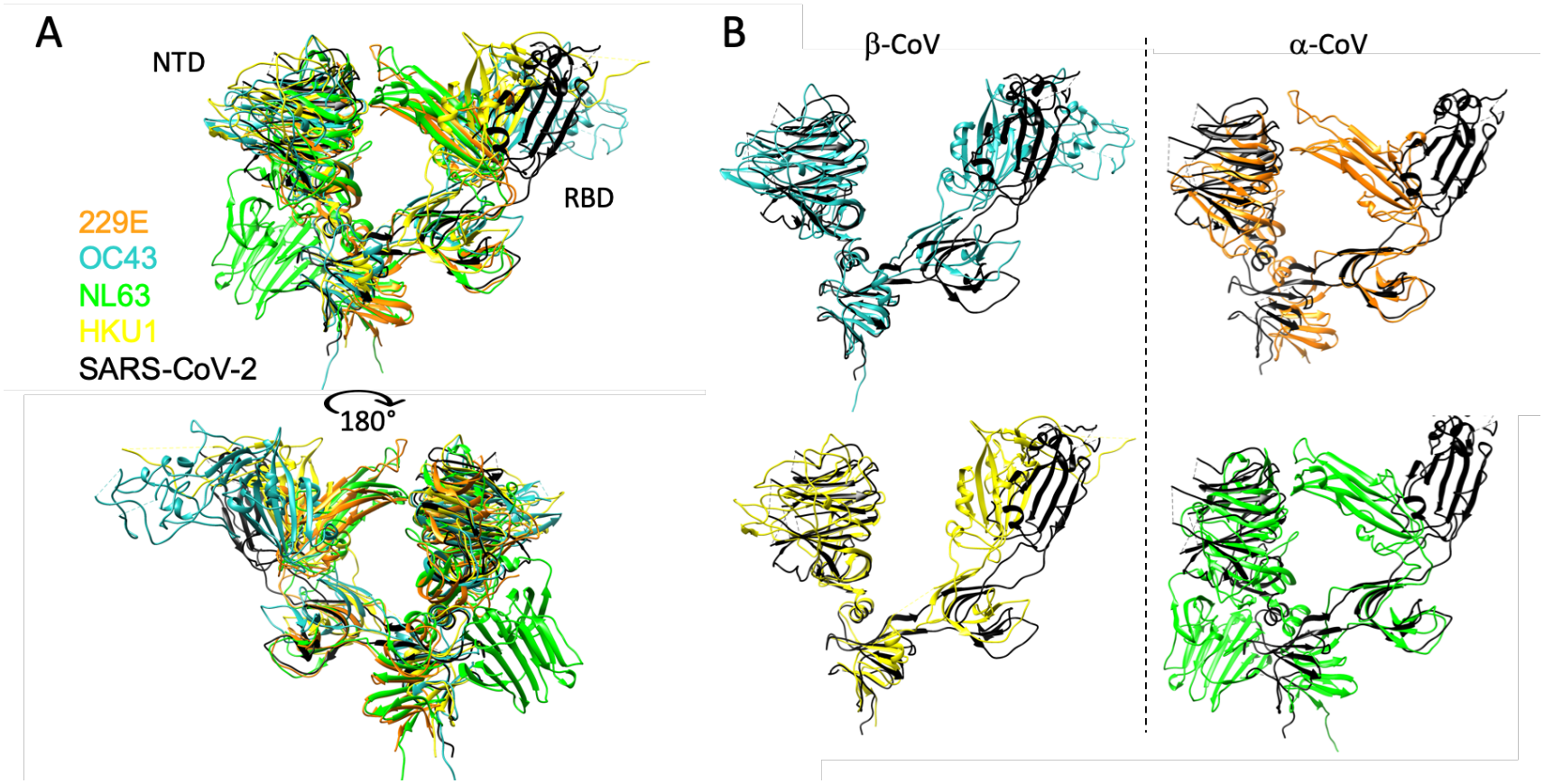

Supplemental Figure 1. Structural differences between the S1 domain of SARS-CoV-2 and endemic strains. A. Structural models of the NTD and RBD as ribbons, colored by strain: SARS-CoV-2 (black), 229E (orange), OC43 (blue), NL63 (green), and HKU1 (yellow). Structural alignments were restricted to the residues of the S1 domain. Right-alignments between SARS-CoV2 and the endemic S1 domains shown individually rather than overlayed, with β-CoV at left, and α-CoV at right.

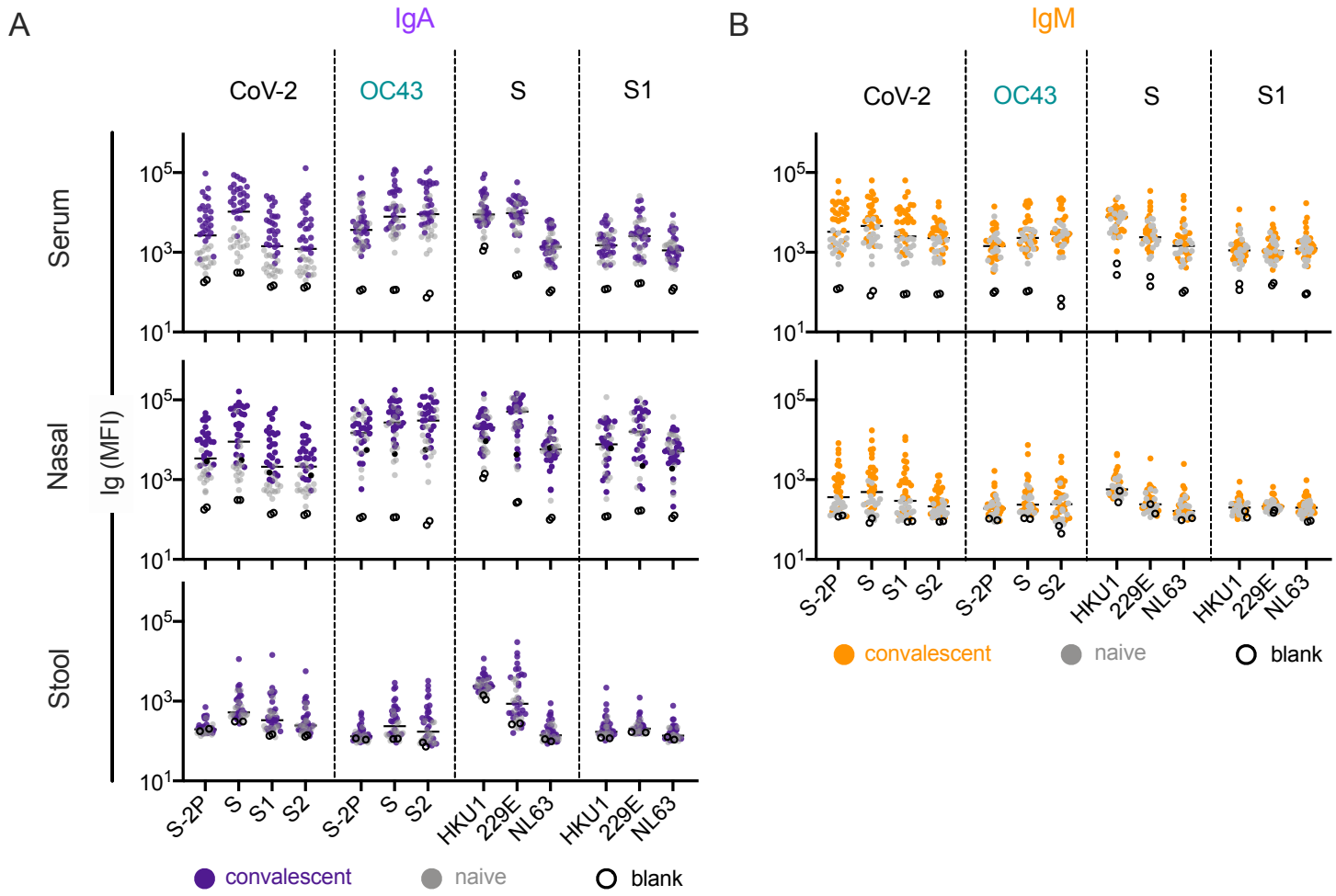

Supplemental Figure 2. IgA and IgM responses in the DHMC cohort. **A-B**. IgA (**A**) and IgM (**B**) responses in serum (top), nasal wash (middle) and stool (bottom) across antigens from CoV-2, OC43, and other endemic CoV S, and S1 proteins. Samples from naïve subjects are indicated in gray, SARS-CoV-2 convalescents at one month post infection in color, and buffer blanks in hollow circles.

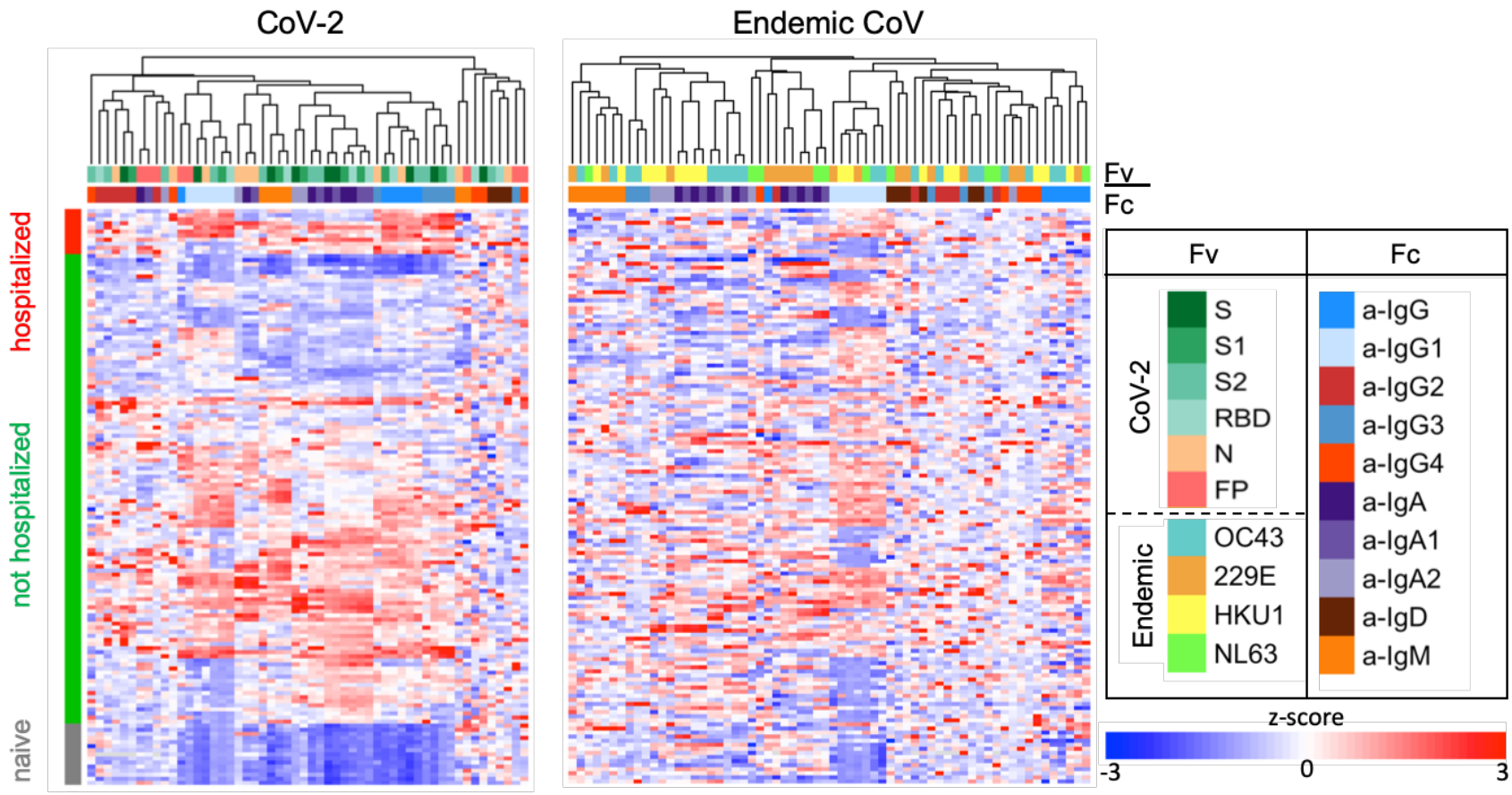

Supplemental Figure 3. Antibody responses in the JHMI cohort. Heatmap of filtered and hierarchically clustered features and within subject groups according to infection and hospitalization status. Ab responses to SARS CoV-2 features are shown on the left and those specific to endemic CoV on the right. Responses were scaled and centered within features and the scale was truncated at +/- 3 SD. Antigen specificity (Fv) and Fc characteristics (Fc) are indicated in the color bars.

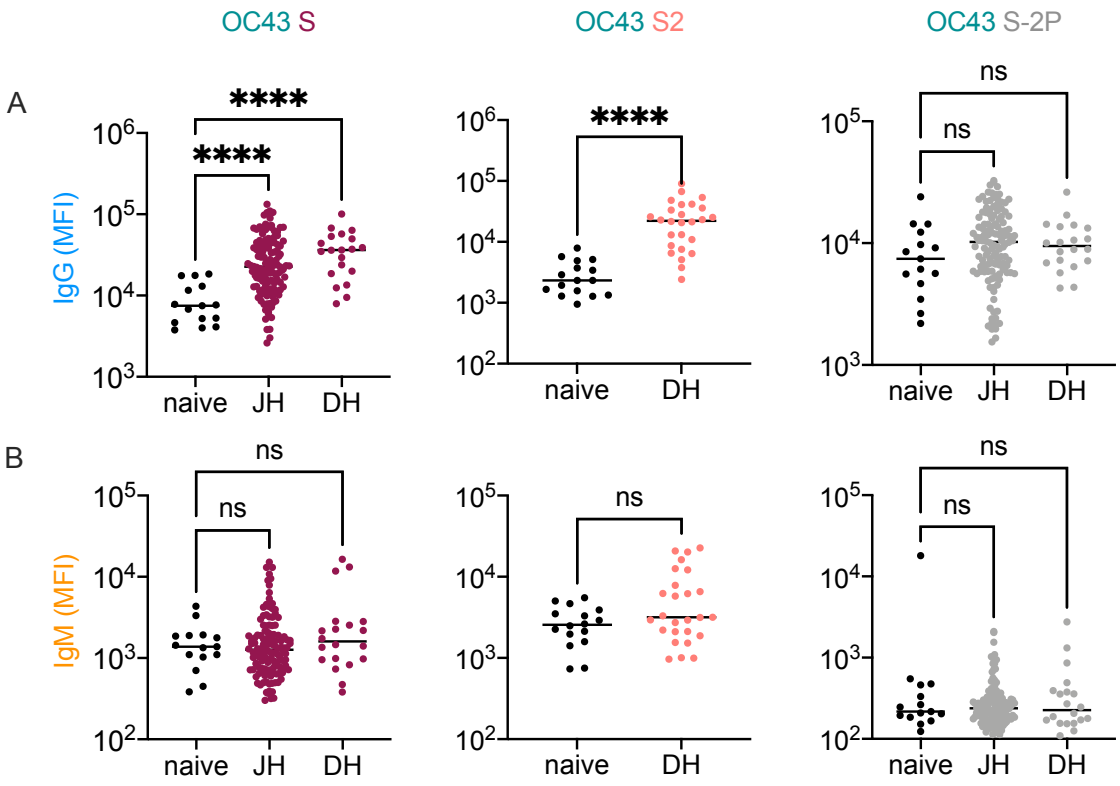

Supplemental Figure 4. Elevated IgG but not IgM responses to endemic CoV in convalescent cohorts. **A-B**. Comparison between IgG (**A**) and IgM (**B**) levels in naïve, DHMC (DH), and JHMI (JH) cohort samples to OC43 S, OC43 S2, and OC43 S-2P. Significant differences were defined by ANOVA with Dunnett's correction (****p<0.0001).

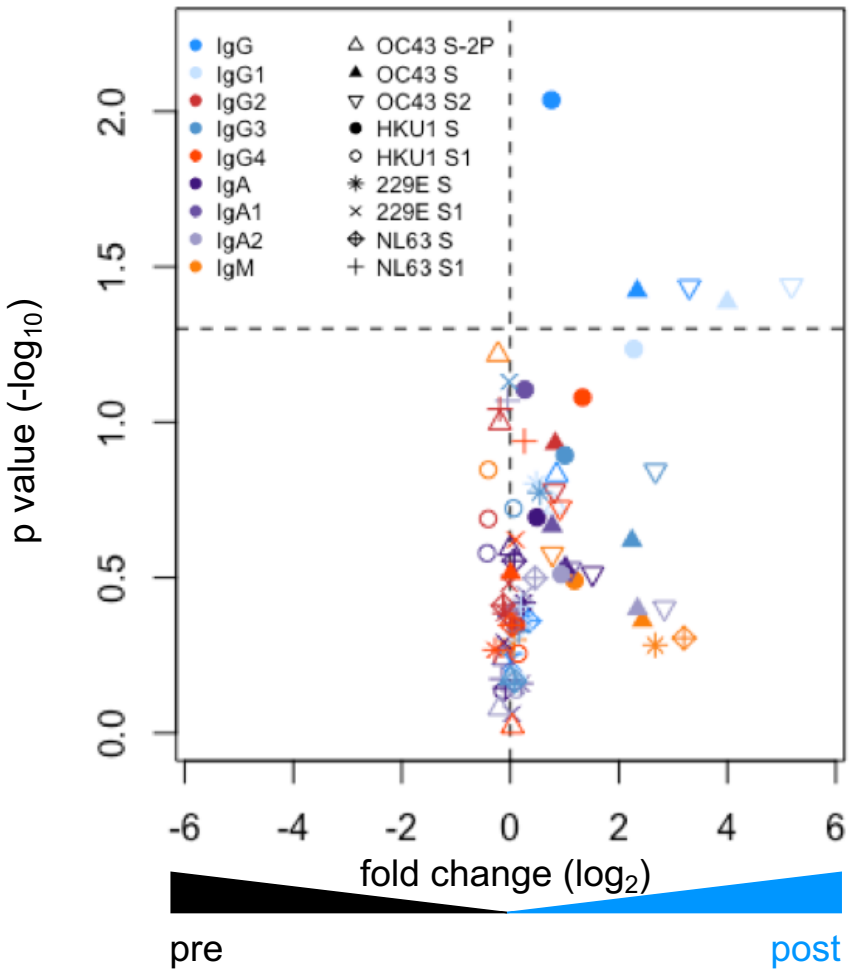

Supplemental Figure 5. Elevated responses to endemic CoV in the pre- and post-infection cohort. Volcano plot of fold change and significance (paired t test) of differences between antibody responses observed in convalescent subjects in the pre- and post-infection cohort. Dotted horizontal line indicates unadjusted p = 0.05. Each symbol represents an antibody response feature, with Fc domain characteristics represented by color and Fv antigen-specificity indicated by shape.

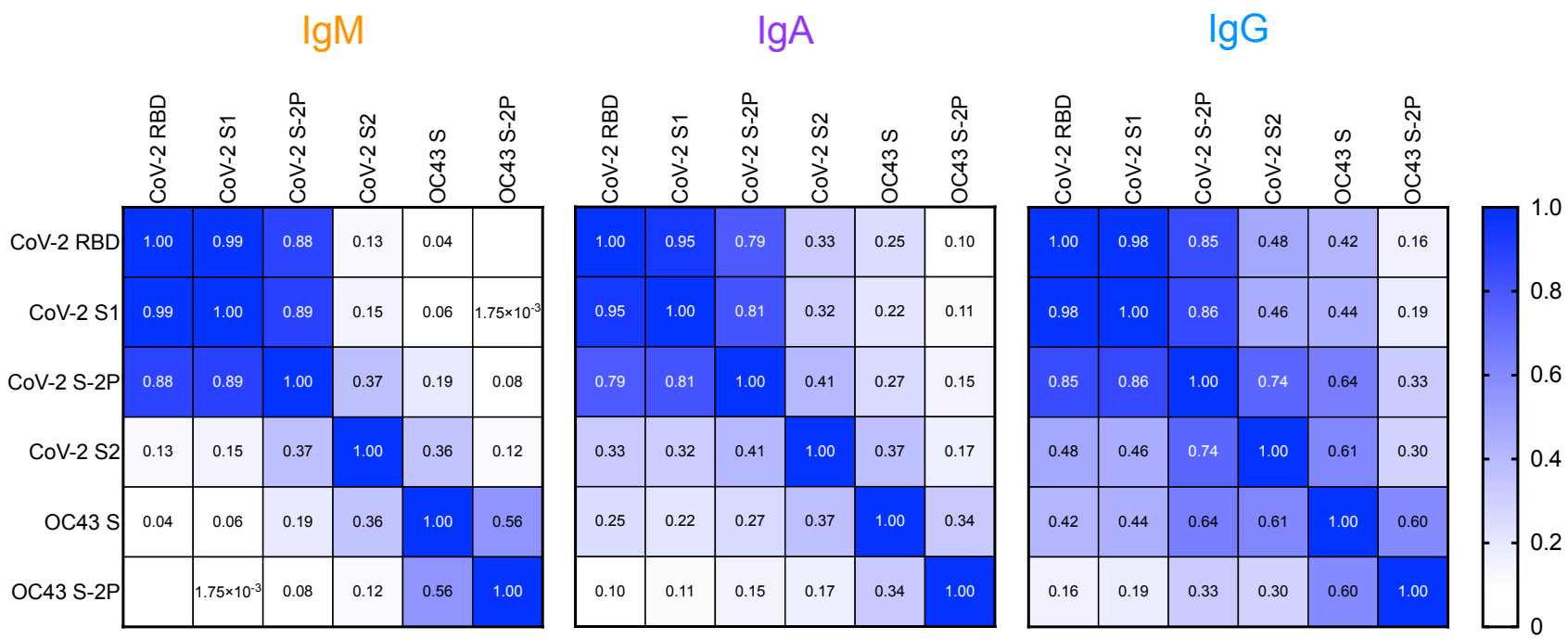

Supplemental Figure 6. Correlative relationships between SARS-CoV-2- and OC43-specific antibody responses in the JHMI cohort by isotype. Heatmap of Pearson correlation coefficients observed among SARS-CoV-2- and OC43-specific IgM (left), IgA (center), and IgG (right) isotypes.

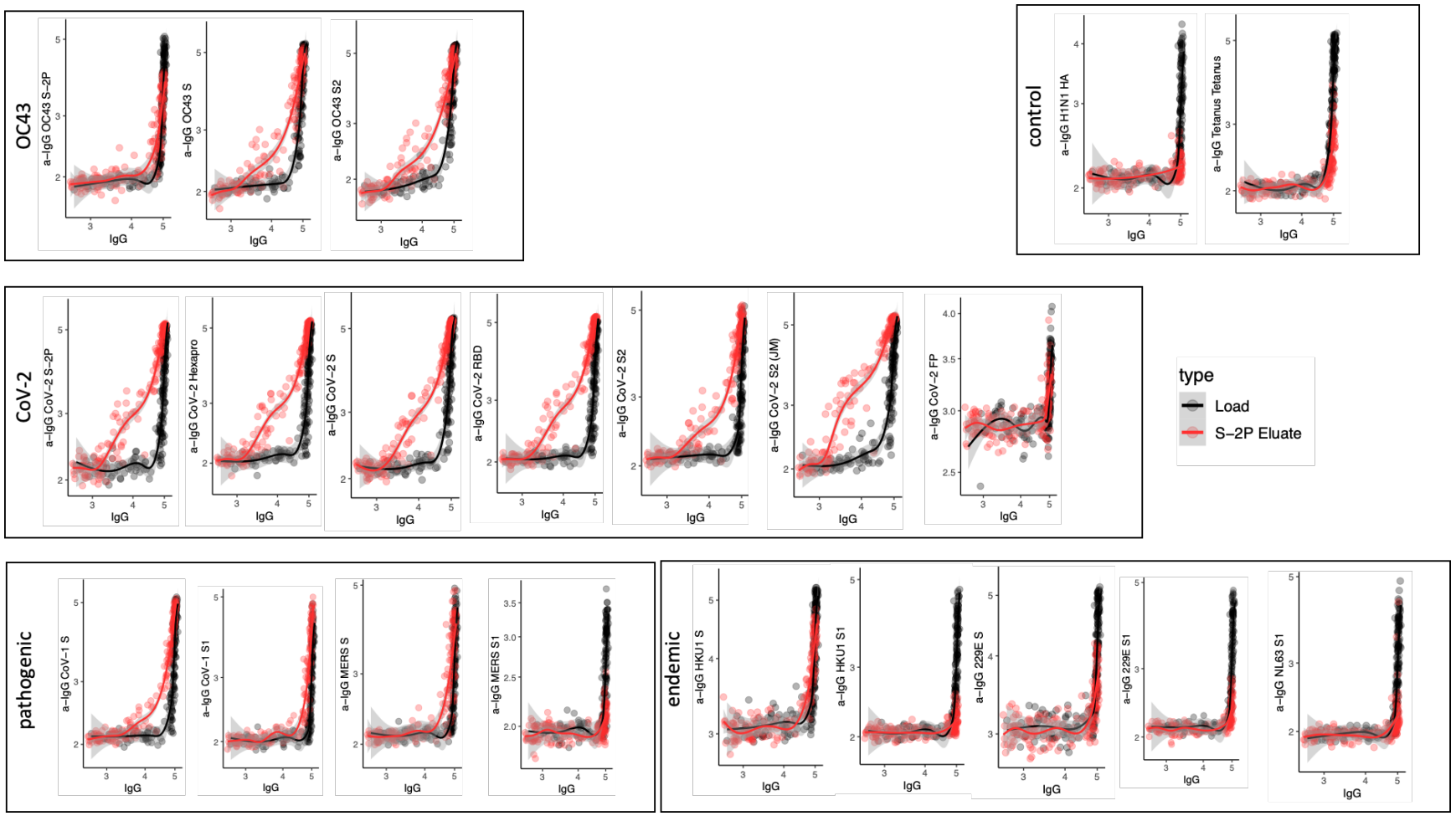

Supplemental Figure 7: Cross-reactivity of SARS-CoV-2 S-2P specific IgG. Antigen binding profiles of IgG in unfractionated serum (load, black) and affinity-purified CoV-2 S-2P- (eluate, red) fractions from 30 SARS-CoV-2 convalescent subjects across OC43, control, CoV-2, pathogenic CoV, and other endemic CoV. Y-axis depicts binding signal for indicated antigen specificity, x-axis depicts signal from total IgG quantitation.

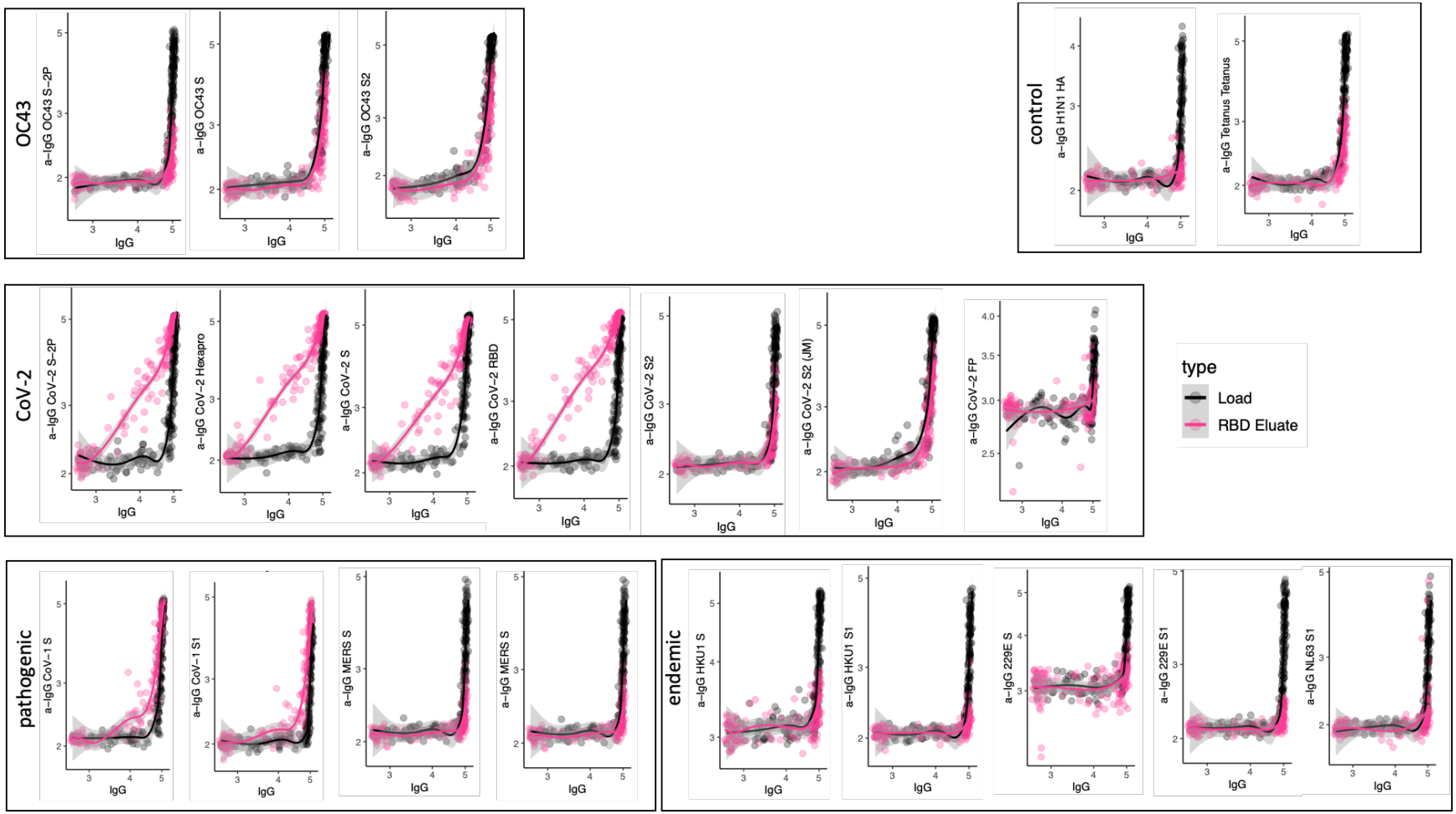

Supplemental Figure 8: Cross-reactivity of SARS-CoV-2 RBD specific IgG. Antigen binding profiles of IgG in unfractionated serum (load, black) and affinity-purified CoV-2 RBD- (eluate, pink) fractions from 30 SARS-CoV-2 convalescent subjects across OC43, control, CoV-2, pathogenic CoV, and other endemic CoV. Y-axis depicts binding signal for indicated antigen specificity, x-axis depicts signal from total IgG quantitation.

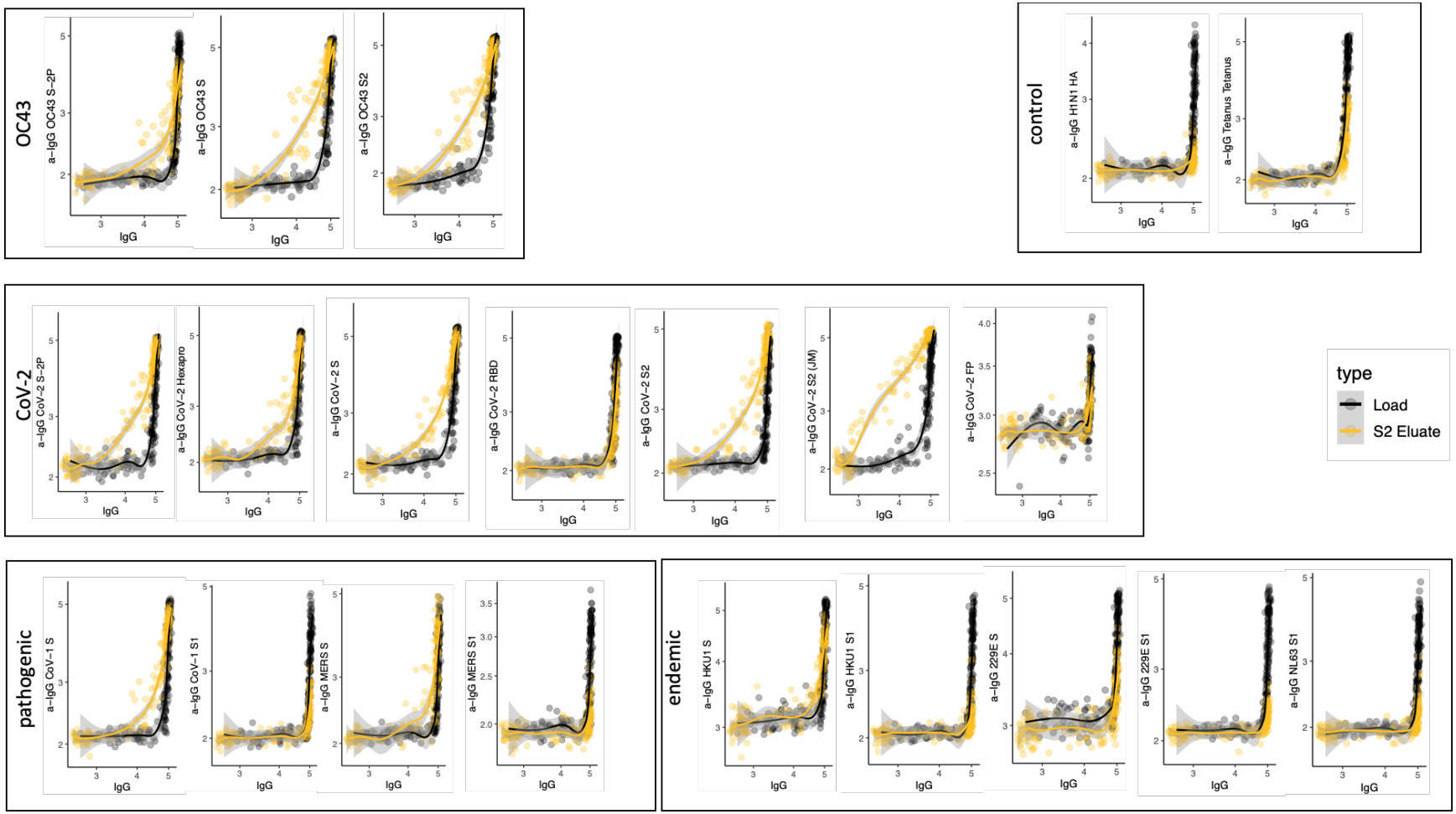

Supplemental Figure 9: Cross-reactivity of SARS-CoV-2 S2 specific IgG. Antigen binding profiles of IgG in unfractionated serum (load, black) and affinity-purified CoV-2 S2- (eluate, yellow) fractions from 30 SARS-CoV-2 convalescent subjects across OC43, control, CoV-2, pathogenic CoV, and other endemic CoV. Y-axis depicts binding signal for indicated antigen specificity, x-axis depicts signal from total IgG quantitation.

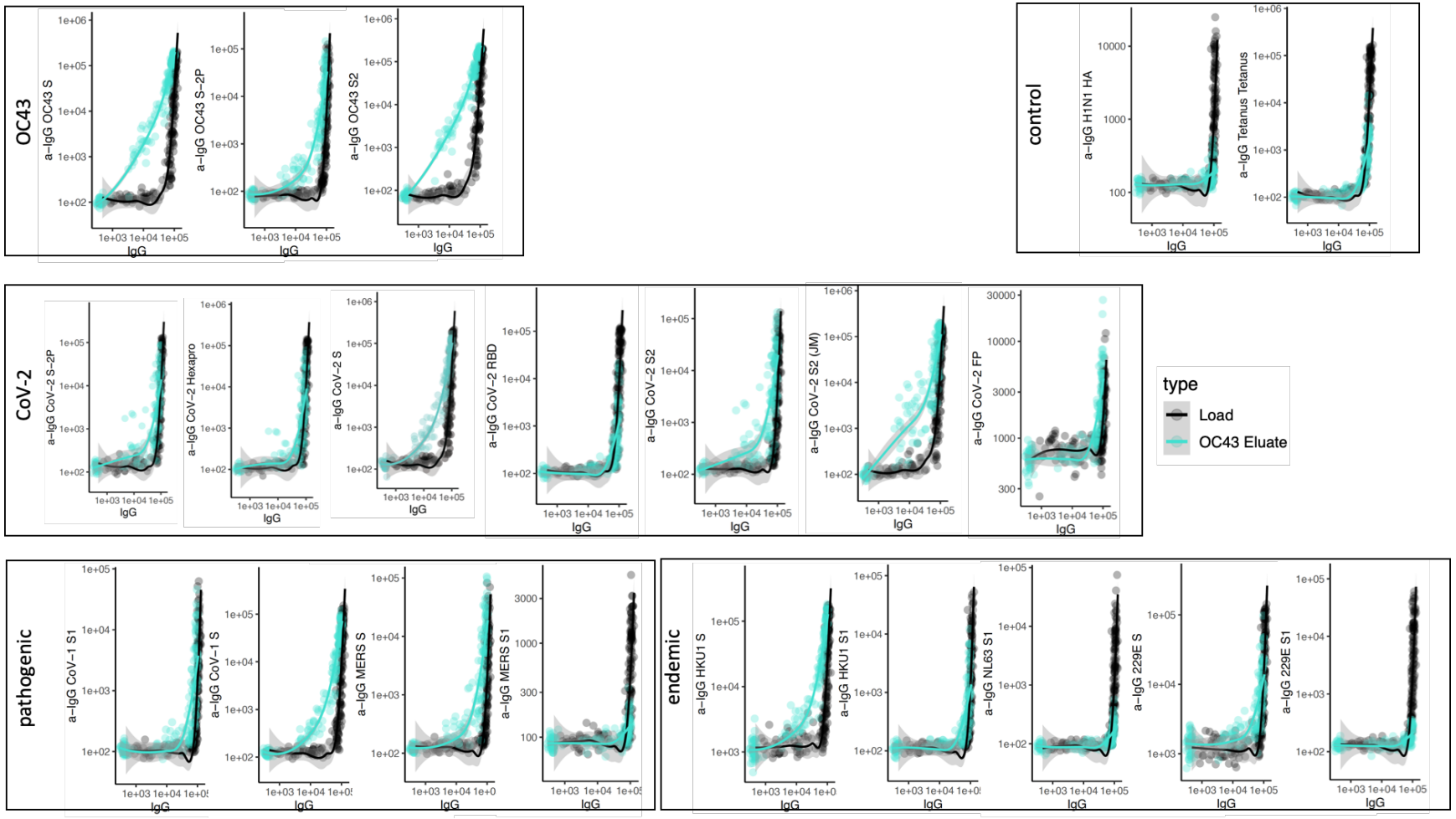

Supplemental Figure 10: Cross-reactivity of OC43 S specific IgG. Antigen binding profiles of IgG in unfractionated serum (load, black) and affinity-purified OC43 S- (eluate teal) fractions from 30 SARS-CoV-2 convalescent subjects across OC43, control, CoV-2, pathogenic CoV, and other endemic CoV. Y-axis depicts binding signal for indicated antigen specificity, x-axis depicts signal from total IgG quantitation.

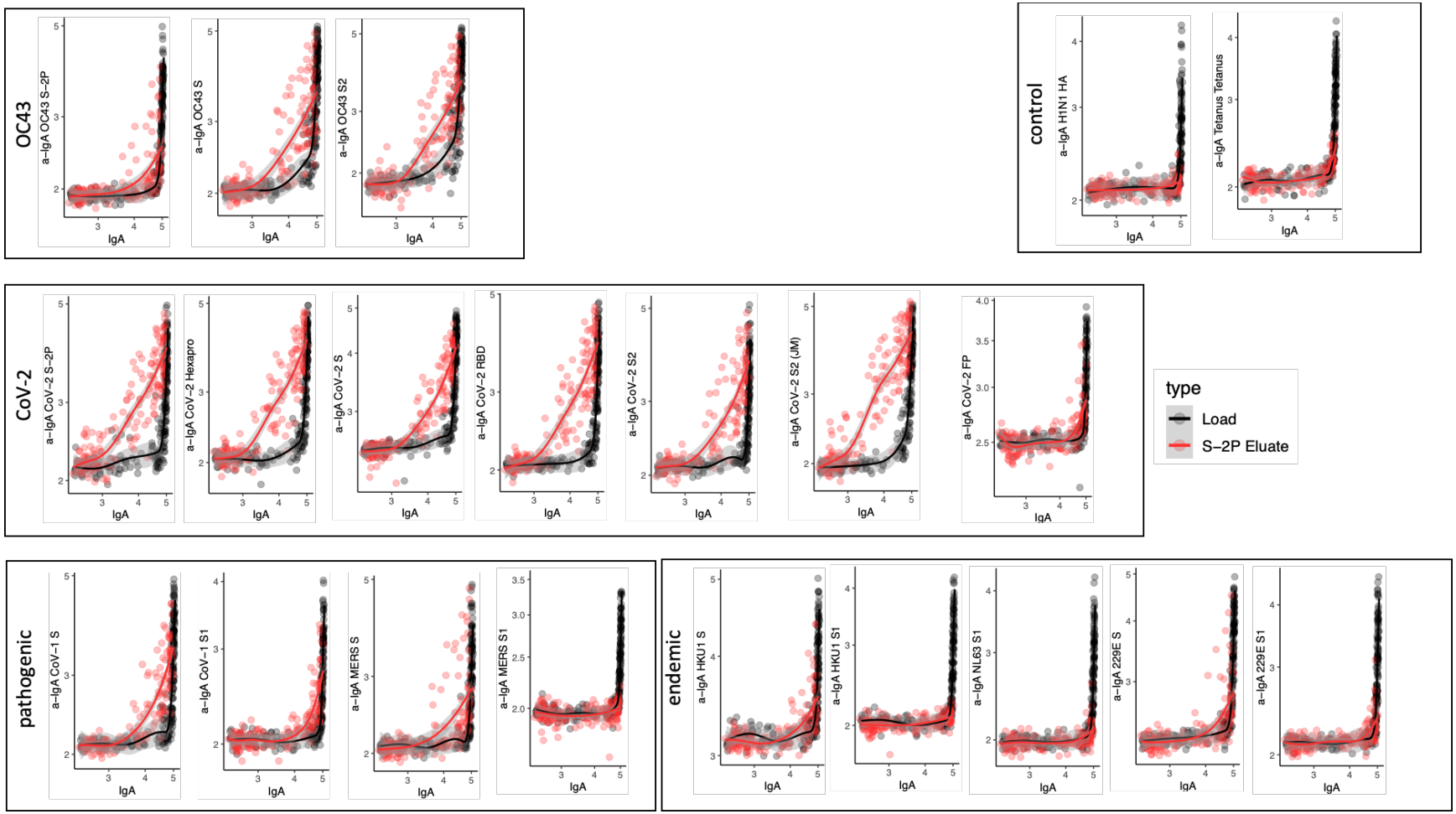

Supplemental Figure 11: Cross-reactivity of SARS-CoV-2 S-2P specific IgA. Antigen binding profiles of IgA in unfractionated serum (load, black) and affinity-purified CoV-2 S-2P- (eluate, red) fractions from 30 SARS-CoV-2 convalescent subjects across OC43, control, CoV-2, pathogenic CoV, and other endemic CoV. Y-axis depicts binding signal for indicated antigen specificity, x-axis depicts signal from total IgA quantitation.

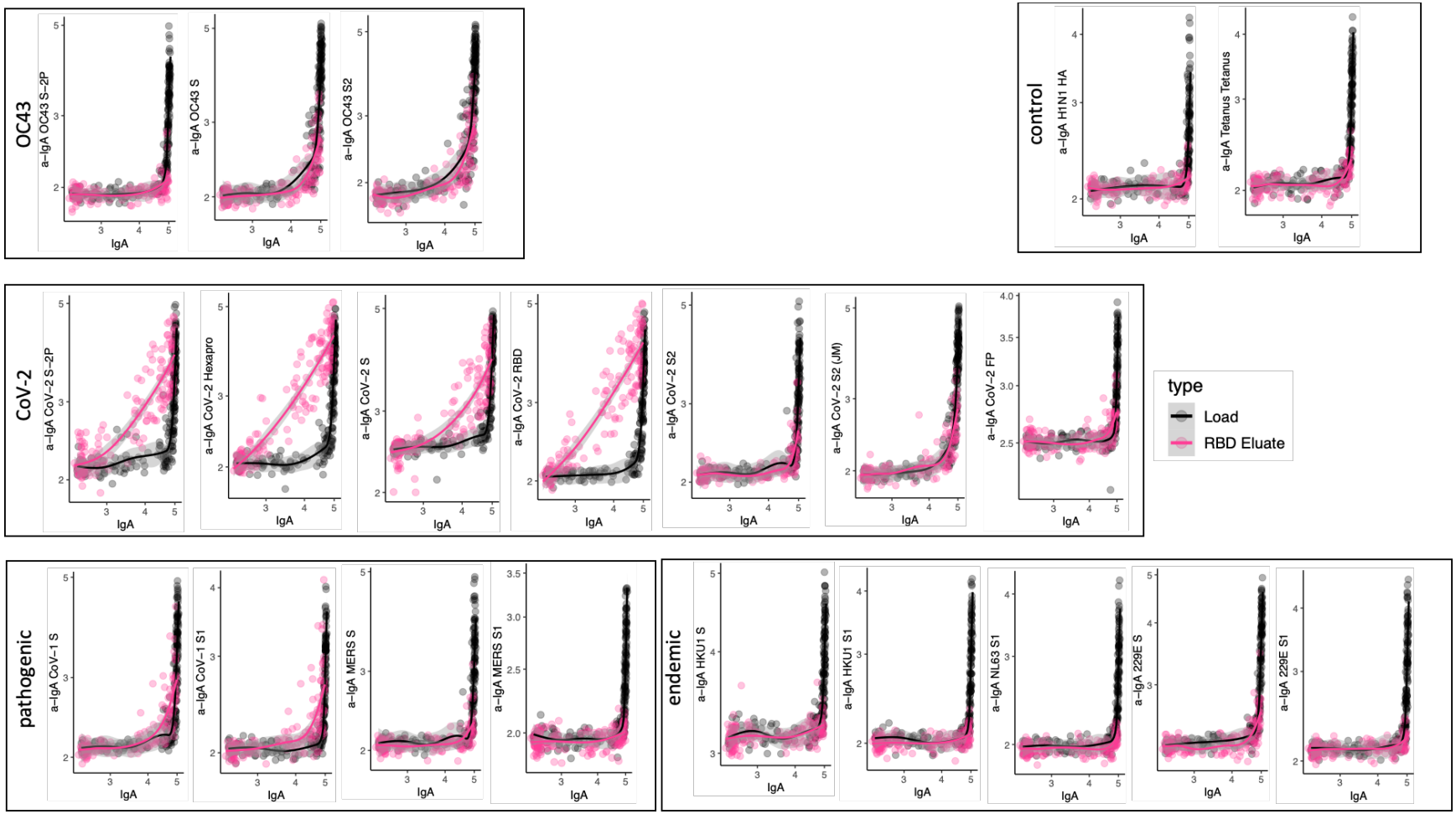

Supplemental Figure 12: Cross-reactivity of SARS-CoV-2 RBD specific IgA. Antigen binding profiles of IgA in unfractionated serum (load, black) and affinity-purified CoV-2 RBD- (eluate, pink) fractions from 30 SARS-CoV-2 convalescent subjects across OC43, control, CoV-2, pathogenic CoV, and other endemic CoV. Y-axis depicts binding signal for indicated antigen specificity, x-axis depicts signal from total IgA quantitation.

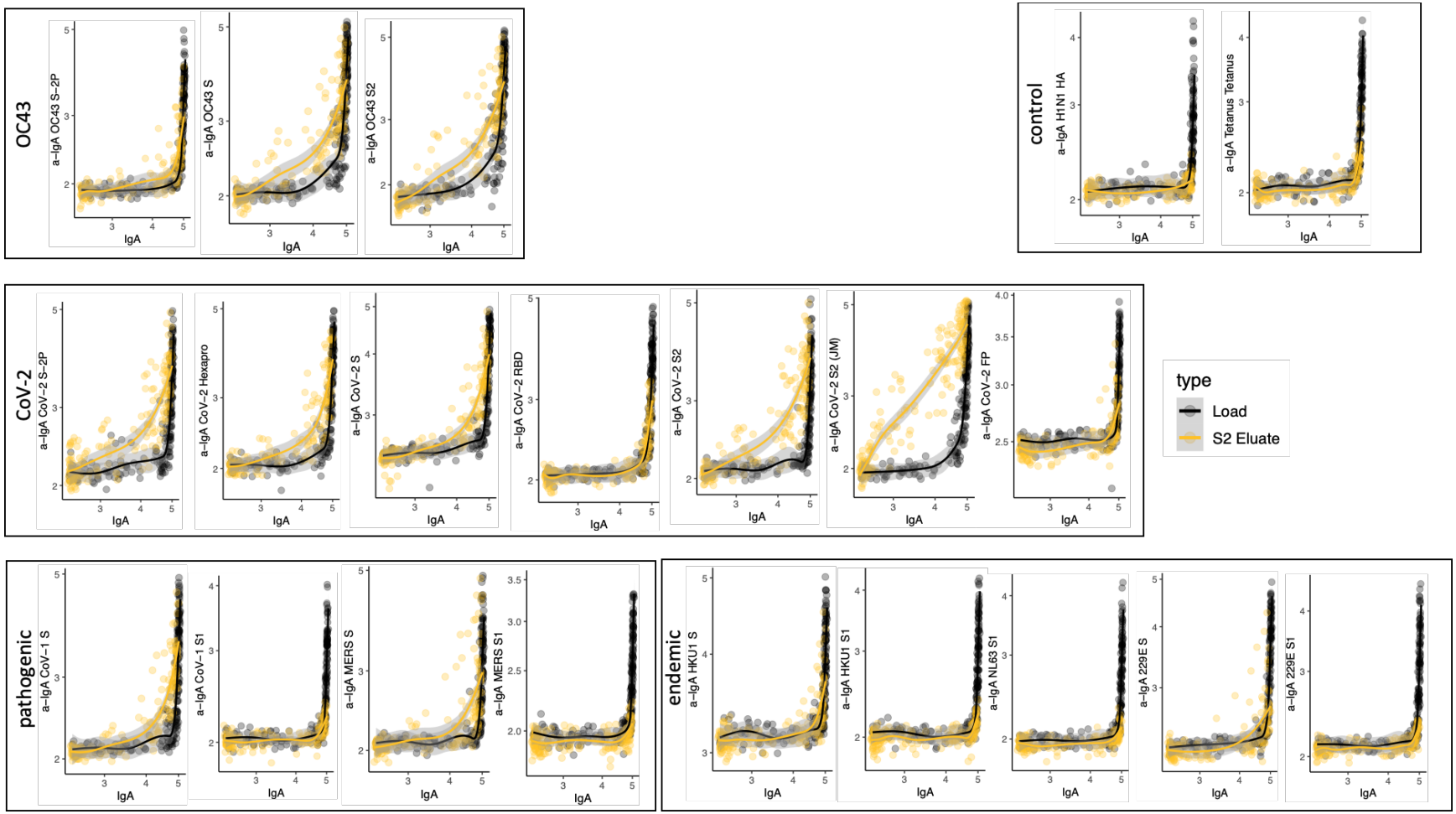

Supplemental Figure 13: Cross-reactivity of SARS-CoV-2 S2 specific IgA. Antigen binding profiles of IgA in unfractionated serum (load, black) and affinity-purified CoV-2 S2- (eluate, yellow) fractions from 30 SARS-CoV-2 convalescent subjects across OC43, control, CoV-2, pathogenic CoV, and other endemic CoV. Y-axis depicts binding signal for indicated antigen specificity, x-axis depicts signal from total IgA quantitation.

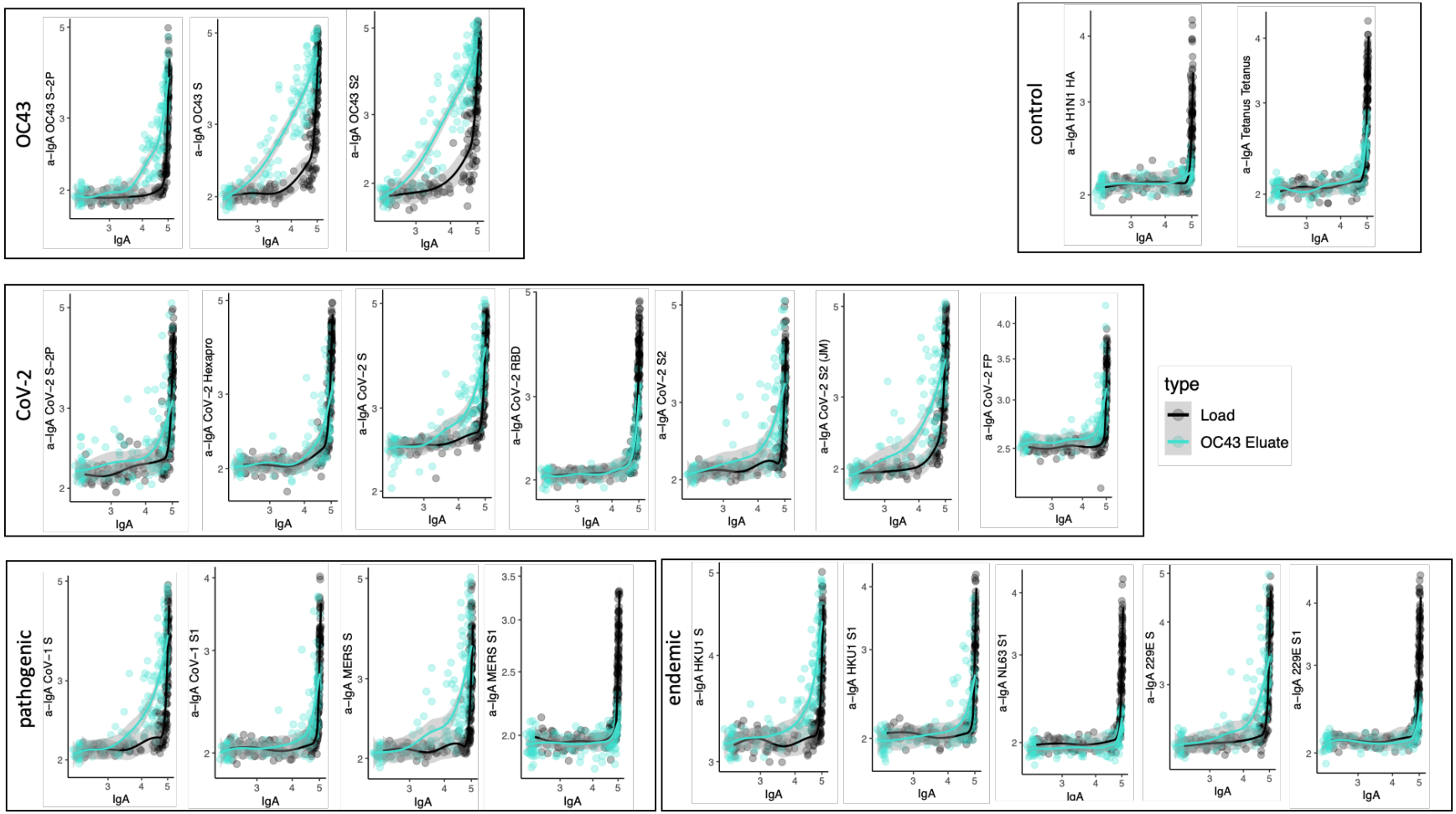

Supplemental Figure 14: Cross-reactivity of OC43 S specific IgA. Antigen binding profiles of IgA in unfractionated serum (load, black) and affinity-purified OC43 S- (eluate teal) fractions from 30 SARS-CoV-2 convalescent subjects across OC43, control, CoV-2, pathogenic CoV, and other endemic CoV. Y-axis depicts binding signal for indicated antigen specificity, x-axis depicts signal from total IgA quantitation.

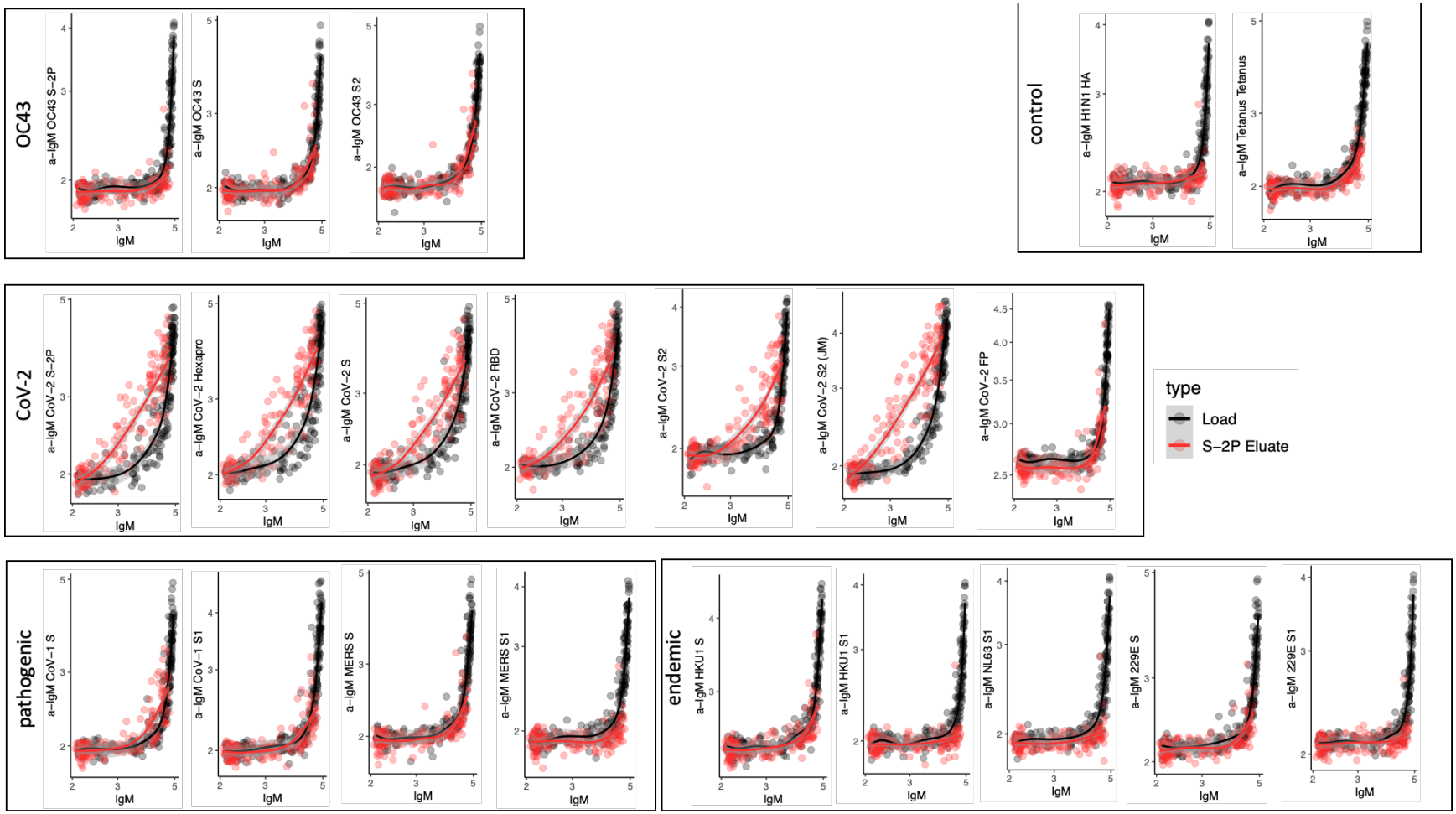

Supplemental Figure 15: Cross-reactivity of SARS-CoV-2 S-2P specific IgM. Antigen binding profiles of IgM in unfractionated serum (load, black) and affinity-purified CoV-2 S-2P- (eluate, red) fractions from 30 SARS-CoV-2 convalescent subjects across OC43, control, CoV-2, pathogenic CoV, and other endemic CoV. Y-axis depicts binding signal for indicated antigen specificity, x-axis depicts signal from total IgM quantitation.

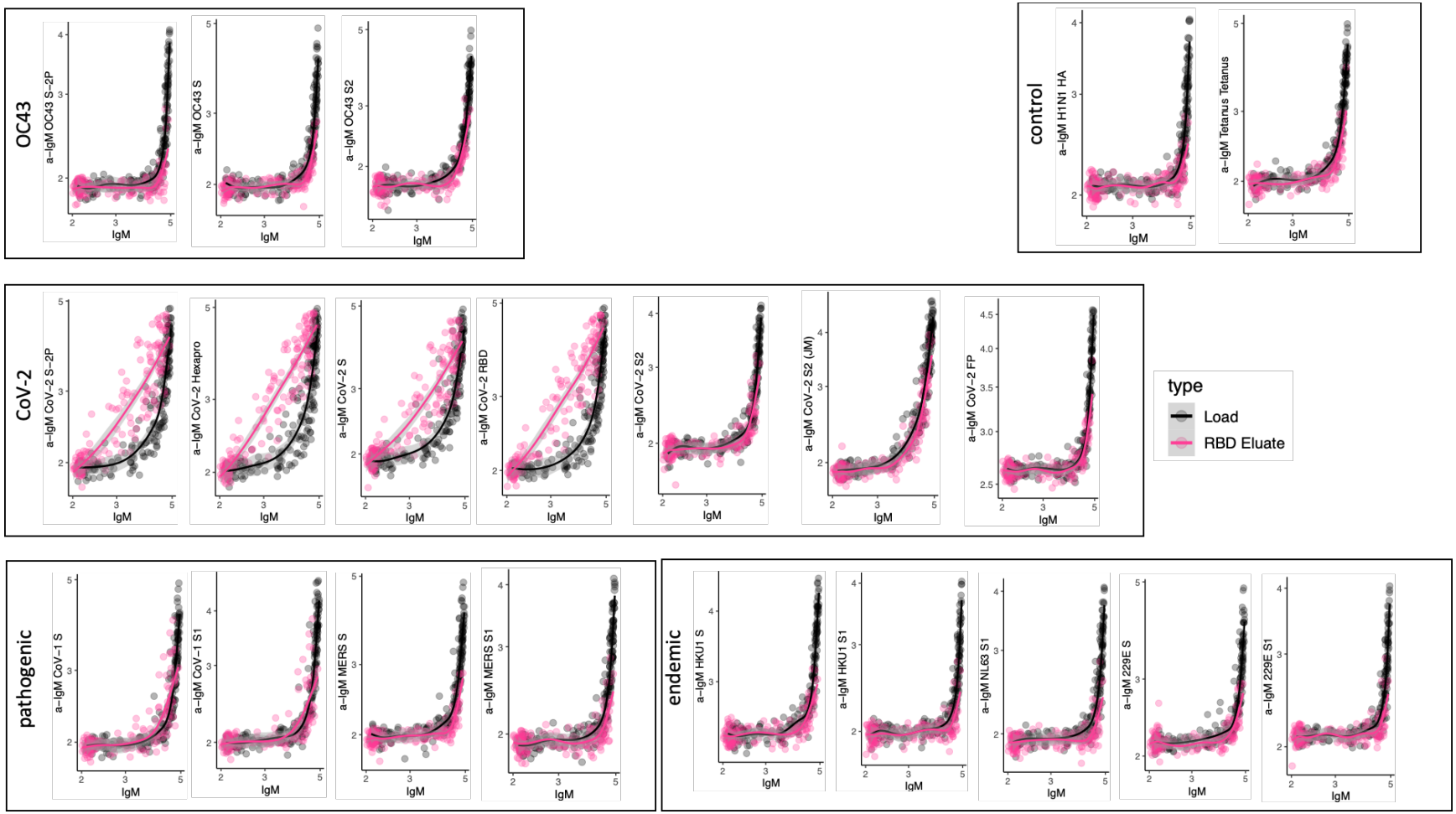

Supplemental Figure 16: Cross-reactivity of SARS-CoV-2 RBD specific IgM. Antigen binding profiles of IgM in unfractionated serum (load, black) and affinity-purified CoV-2 RBD- (eluate, pink) fractions from 30 SARS-CoV-2 convalescent subjects across OC43, control, CoV-2, pathogenic CoV, and other endemic CoV. Y-axis depicts binding signal for indicated antigen specificity, x-axis depicts signal from total IgM quantitation.

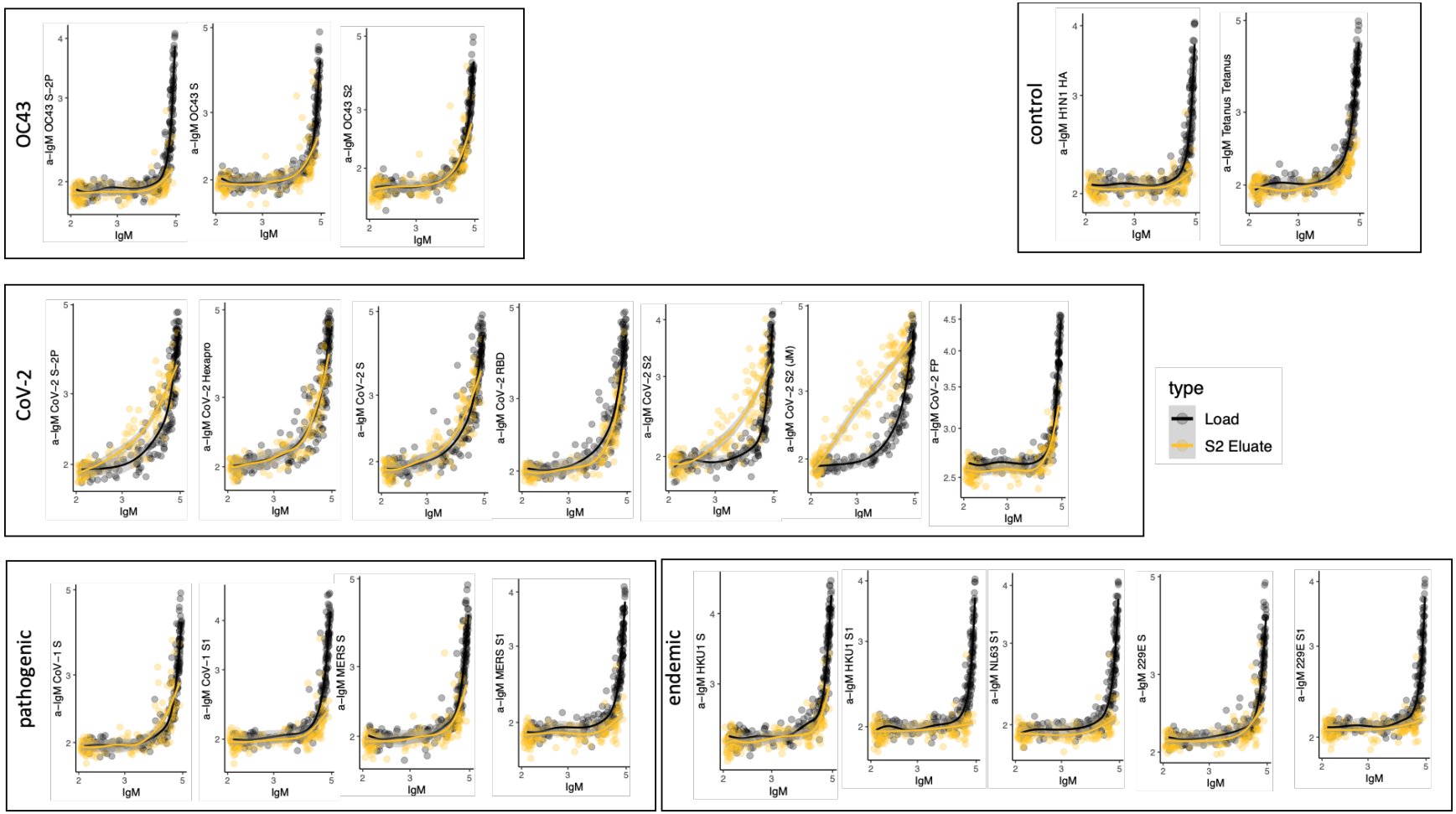

Supplemental Figure 17: Cross-reactivity of SARS-CoV-2 S2 specific IgM. Antigen binding profiles of IgM in unfractionated serum (load, black) and affinity-purified CoV-2 S2- (eluate, yellow) fractions from 30 SARS-CoV-2 convalescent subjects across OC43, control, CoV-2, pathogenic CoV, and other endemic CoV. Y-axis depicts binding signal for indicated antigen specificity, x-axis depicts signal from total IgM quantitation.

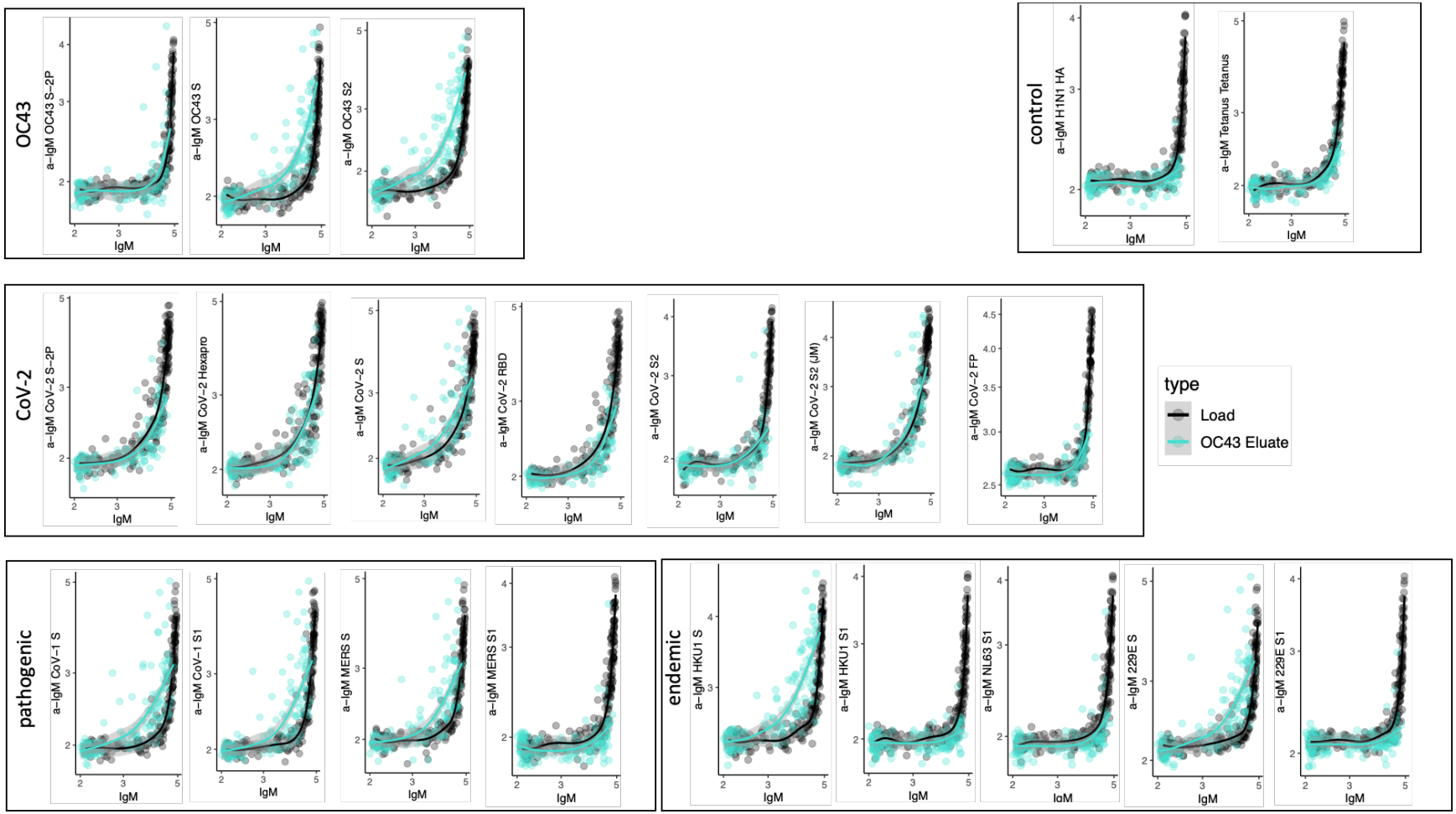

Supplemental Figure 18: Cross-reactivity of OC43 S specific IgM. Antigen binding profiles of IgM in unfractionated serum (load, black) and affinity-purified OC43 S- (eluate teal) fractions from 30 SARS-CoV-2 convalescent subjects across OC43, control, CoV-2, pathogenic CoV, and other endemic CoV. Y-axis depicts binding signal for indicated antigen specificity, x-axis depicts signal from total IgM quantitation.

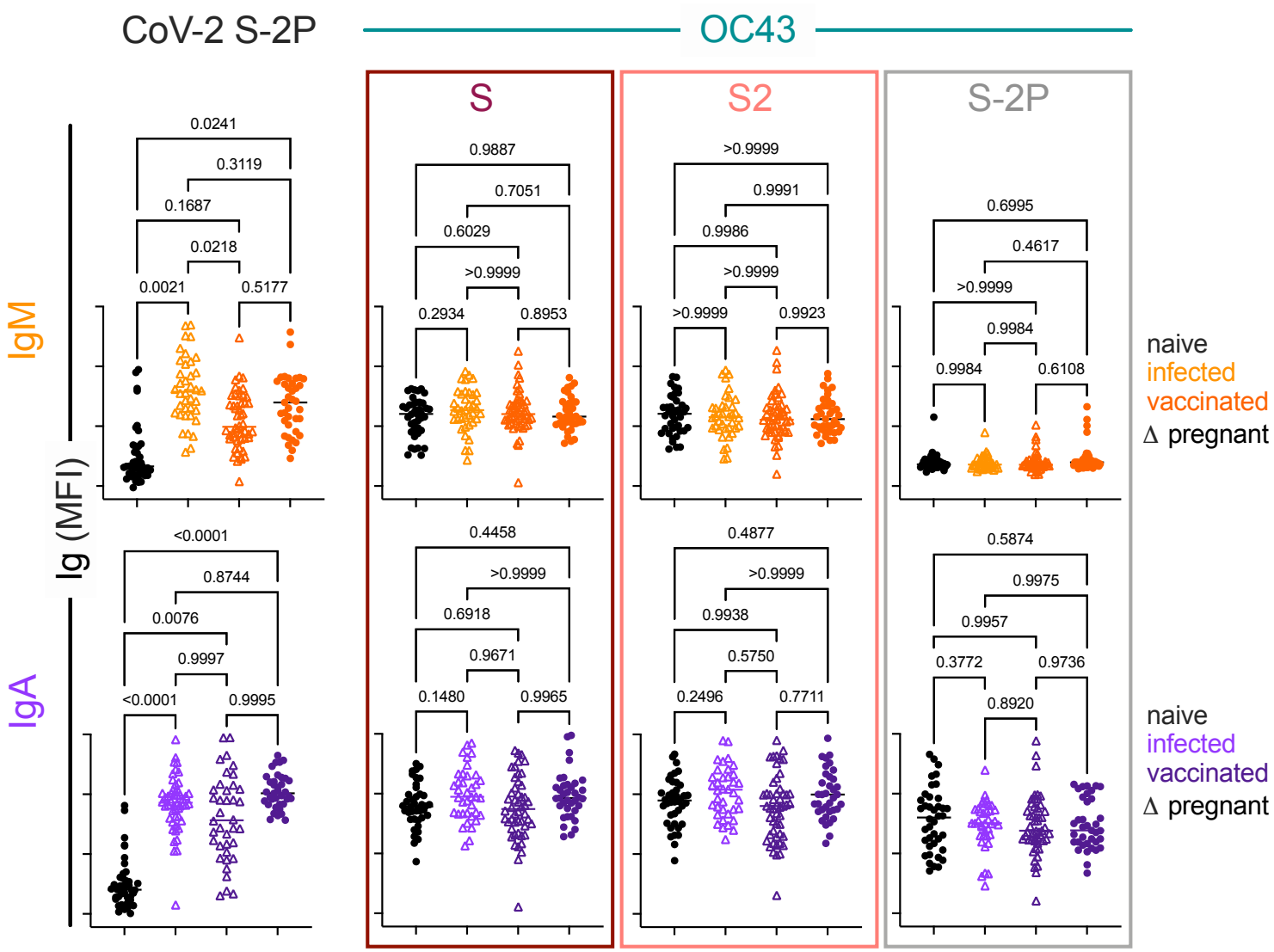

Supplemental Figure 19. IgA and IgM responses among naïve subjects, infected pregnant women, vaccinated adults, and vaccinated pregnant women. Box plots of IgM (top) and IgA (bottom) responses to SARS CoV-2 S-2P (left) and OC43 (right) S, S2, and S-2P. Statistical significance by ANOVA with Dunnett's correction.

Supplemental Table 1. Coronavirus structures. Spike protein information used to construct structural visualizations. PDB: Protein Data Bank; EM: electron microscopy.

	PDB	Type	Resolution (Å)	Format
SARS-CoV-2	6XKL	EM	3.21	Trimer
229E	6U7H	EM	3.1	Trimer
OC43	6OHW	EM	2.9	Trimer
NL63	5SZS	EM	3.4	Trimer
HKU1	5I08	EM	4.04	Trimer
SARS-CoV-2 Closed	6X6P	EM	3.22	Trimer

Supplemental Table 2. Fc detection and antigen reagents

Antigen	**Source**
H1N1 HA1	Immune Technology IT-003-00110p
HSV gE	Immune Technology IT-005-005p
Tetanus	Sigma 676570-37-9
SARS CoV-2 N	Immune Technology IT-002-033Ep
SARS CoV-2 FP	New England Peptide
SARS CoV-2 S1	ACRO Biosystems S1N-C52H3-100ug
SARS CoV-2 RBD	BEI Resources NR-52366
SARS CoV-2 S2	Immune Technology IT-002-034p
SARS CoV-2 S-2P	Expressed in Expi 293
SARS-CoV-2 S-6P	Expressed in Expi 293
WIV1 S-2P	Expressed in Expi 293
SARS-CoV-1 S	Sino Biological 40634-V08B
SARS CoV-1 S1	Sino Biological 40150-V08B1
MERS S	Sino Biological
MERS S1	Sino Biological 40069-V08B1
OC43 S	Sino Biological 40607-V08B
OC43 S-2P	Expressed in HEK 293F
OC43 S2	Sino Biological 40069-V08B
229E S1	Sino Biological 40605-V08H
229E S	Sino Biological 40601-V08H
HKU1 S	Sino Biological 40606-V08H
HKU1 S1	Sino Biological 40606-V08H
NL63 S1	Sino Biological 40604-V08H
NL63 S	Sino Biological 40606-V08B
Fc Detection	**Source**
a- IgG	Southern Biotech 1030-09
a-IgG1	Southern Biotech 9054-09
a-IgG2	Southern Biotech 9070-09
a-IgG3	Southern Biotech 9210-09
a-IgG4	Southern Biotech 9200-09
a-IgA	Southern Biotech 2050-09
a-IgA1	Southern Biotech 9130-09
a-IgA2	Southern Biotech 9140-09
a-IgM	Southern Biotech 9020-09